



## Atmospheric temperature changes by volcanic eruptions: GPS radio occultation observations in the 2010 Icelandic and 2011 Chilean cases

Ikuya Okazaki<sup>1</sup>, Kosuke Heki<sup>\*</sup>

Department of Natural History Sciences, Hokkaido University, N10 W8, Kita-ku, Sapporo-city, 060-0810, Japan

### ARTICLE INFO

#### Article history:

Received 20 April 2012

Accepted 24 August 2012

Available online 31 August 2012

#### Keywords:

Iceland

Chile

Volcanic eruption

2010

2011

GPS

Temperature change

Occultation

### ABSTRACT

Volcanic plumes modify atmospheric temperatures. Wang et al. (2009) reported localized temperature changes associated with the Mt Chaiten eruption in May 2008 using the deviation of GPS radio occultation temperature data from the NCEP global forecast system model. On 14 April 2010, a large scale eruption started under the glacier Eyjafjallajökull in Southern Iceland, and Puyehue-Cordón Caulle (Puyehue), in Chile, started eruption on 4 June, 2011. Here we study instantaneous and localized temperature changes with these two eruptions following the method of Wang et al. (2009). Post-eruption negative temperature anomalies at the 250 hPa plane were clearly observed in the Eyjafjallajökull eruption. In the Puyehue eruption, however, such anomalies were not so clear due possibly to insufficient accuracy of the forecast model. By comparing the temperature profiles in the downwind areas of the two eruptions, we found that significant temperature decreases occurred at ~10.5 and ~11.5 km altitude in the Eyjafjallajökull and the Puyehue cases, respectively. These results generally agree with Wang et al. (2009), but post-eruption temperature changes seem to be influenced by additional factors, e.g. volcanic explosivity and local climatology.

© 2012 Elsevier B.V. All rights reserved.

### 1. Introduction

Atmospheric temperatures are influenced by volcanic plumes. The Mt Pinatubo eruption in June 1991 caused a 0.4° decrease of the global mean tropospheric temperature in 1992 (McCormick et al., 1995). Wang et al. (2009) reported localized temperature changes caused by the volcanic plume in the Mt Chaiten eruption in May 2008 detected as the difference of the temperature data of the Global Positioning System Radio Occultation (GPS-RO) observations by the FORMOSAT-3/Constellation Observing System for Meteorology, Ionosphere and Climate (COSMIC) from the NCEP (National Centers for Environmental Prediction) Global Forecast System (GFS) model temperatures.

On 14 April 2010, a large scale eruption started under the glacier of Eyjafjallajökull in Southern Iceland (Global Volcanism Program, 2010). The large ash plume spread and covered northern Europe. In the explosive eruption of the Puyehue-Cordón Caulle, Chile, on 4 June 2011, the plume drifted round the southern hemisphere and reached Australia in a week (Global Volcanism Program, 2011). Here we use the FORMOSAT-3/COSMIC (FS3/C) data following the approach of Wang et al. (2009), and study instantaneous and localized temperature changes associated with these two eruptions.

### 2. Data and methods

GPS-RO is a technique to observe phases of microwave signals from GPS satellites near the Earth's horizon with receivers on board low earth orbiters. Changes of the received phases are converted to the vertical profiles of the atmospheric refractive indices, which are further converted into quantities such as temperature, water vapor pressure, and ionospheric electron density. FS3/C is composed of six low earth orbiters, and is capable of obtaining up to 2500 profiles per day (Huang et al., 2005). Its spatial resolution is ~1 km or higher in the vertical but 100–300 km in the horizontal plane (Wang and Lin, 2007).

In GPS-RO, temperature profiles are inferred from the observed profiles of atmospheric refractivity. The contribution of moisture to the refractivity is negligible in the upper troposphere and stratosphere (e.g., Wickert, 2004). Comparisons of temperature profiles inferred this way with radiosonde observations suggested that they are accurate to better than 0.6 K at heights 5–15 km (Hajj et al., 2004).

The reference water vapor distribution can be obtained with the one-dimensional variational method using the NCEP GFS model (Anthes et al., 2008). There we used the meteorological condition at 00:00 UTC on the previous day of the eruption as the initial value. Then the contour maps of daily average temperatures on the 250 hPa plane were derived for later days from the model output. These maps were used as the references to discuss post-eruption temperature anomalies. Although the initial NCEP model is derived from various data including those by GPS-RO (<http://www.emc.ncep.noaa.gov/GSF/impl.php>), forecasted models are independent from any data observed after the eruption.

<sup>\*</sup> Corresponding author. Tel.: +81 11 706 3826; fax: +81 11 571 9616.

E-mail address: [heki@mail.sci.hokudai.ac.jp](mailto:heki@mail.sci.hokudai.ac.jp) (K. Heki).

<sup>1</sup> Now at KDDI Corporation.

In order to infer horizontal distributions of the volcanic plumes, we downloaded the data of aerosol optical depths derived from Moderate Resolution Imaging Spectro-radiometer (MODIS) onboard the NASA's Terra and Aqua satellites. The data were available from the Goddard Earth Sciences Data and Information Services Center (GES DISC) (<http://daac.gsfc.nasa.gov/>).

### 3. Results and discussion

#### 3.1. Aerosol observations

Fig. 1a shows the Terra satellite MODIS image of the volcanic plume during 14–15 April 2010, shortly after the eruption of the

Eyjafjallajökull, Iceland. The center of the plume is shifted toward ESE due to winds. The maximum plume height was found to exceed 8 km during 14–16 April (Global Volcanism Program, 2010).

Fig. 1b shows the Aqua satellite MODIS image during 4–6 June 2011, after the eruption of Puyehue, Chile. In spite of the lack of data in the polar region, the plume can be seen to have drifted eastward. The maximum plume height is considered to be 10.7–13.7 km on 4 June (Global Volcanism Program, 2011).

#### 3.2. Temperature anomaly: Eyjafjallajökull

Fig. 2 shows the daily average temperature distributions on the 250 hPa plane from 13 (one day before the eruption) to 16 (two

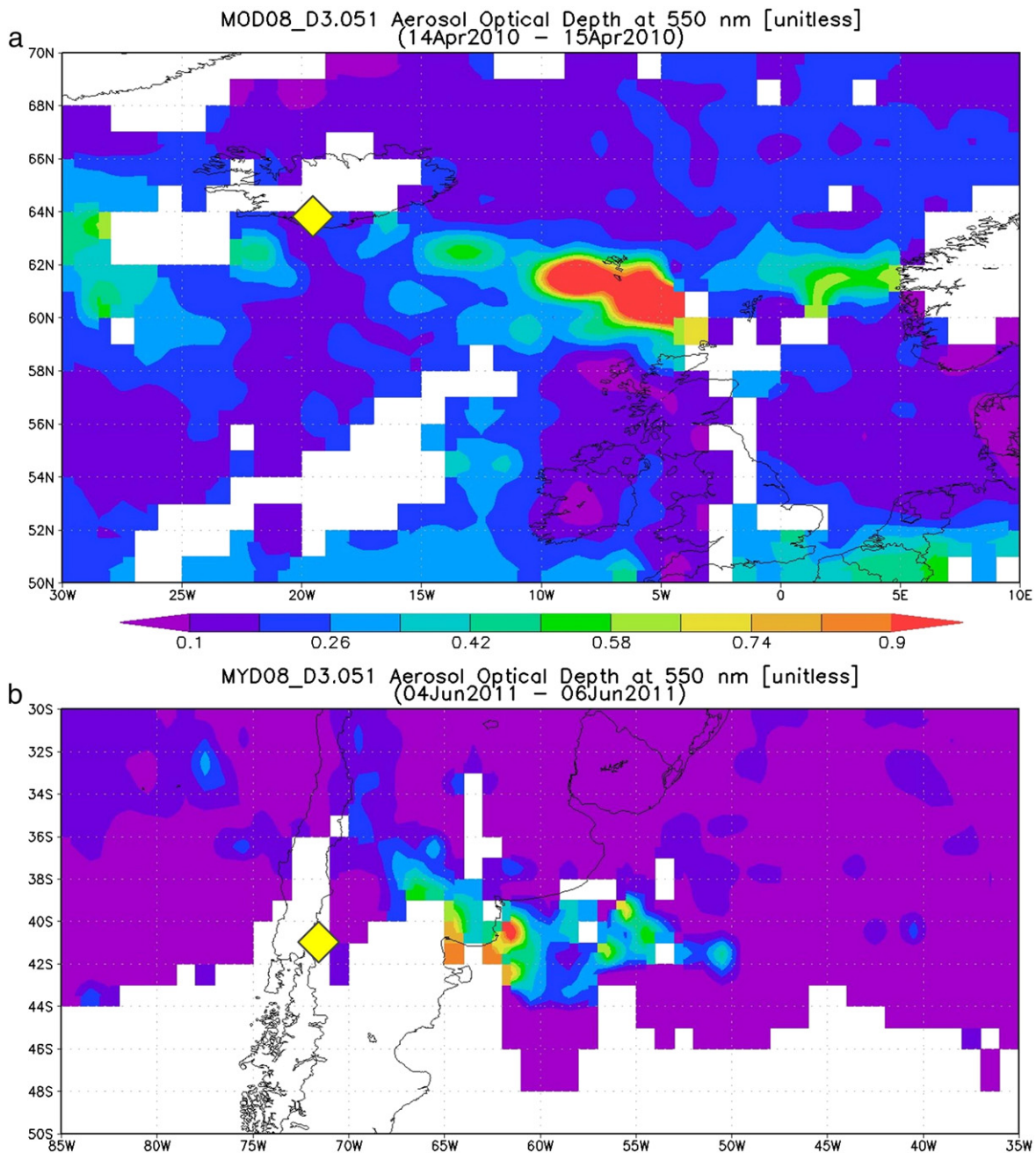
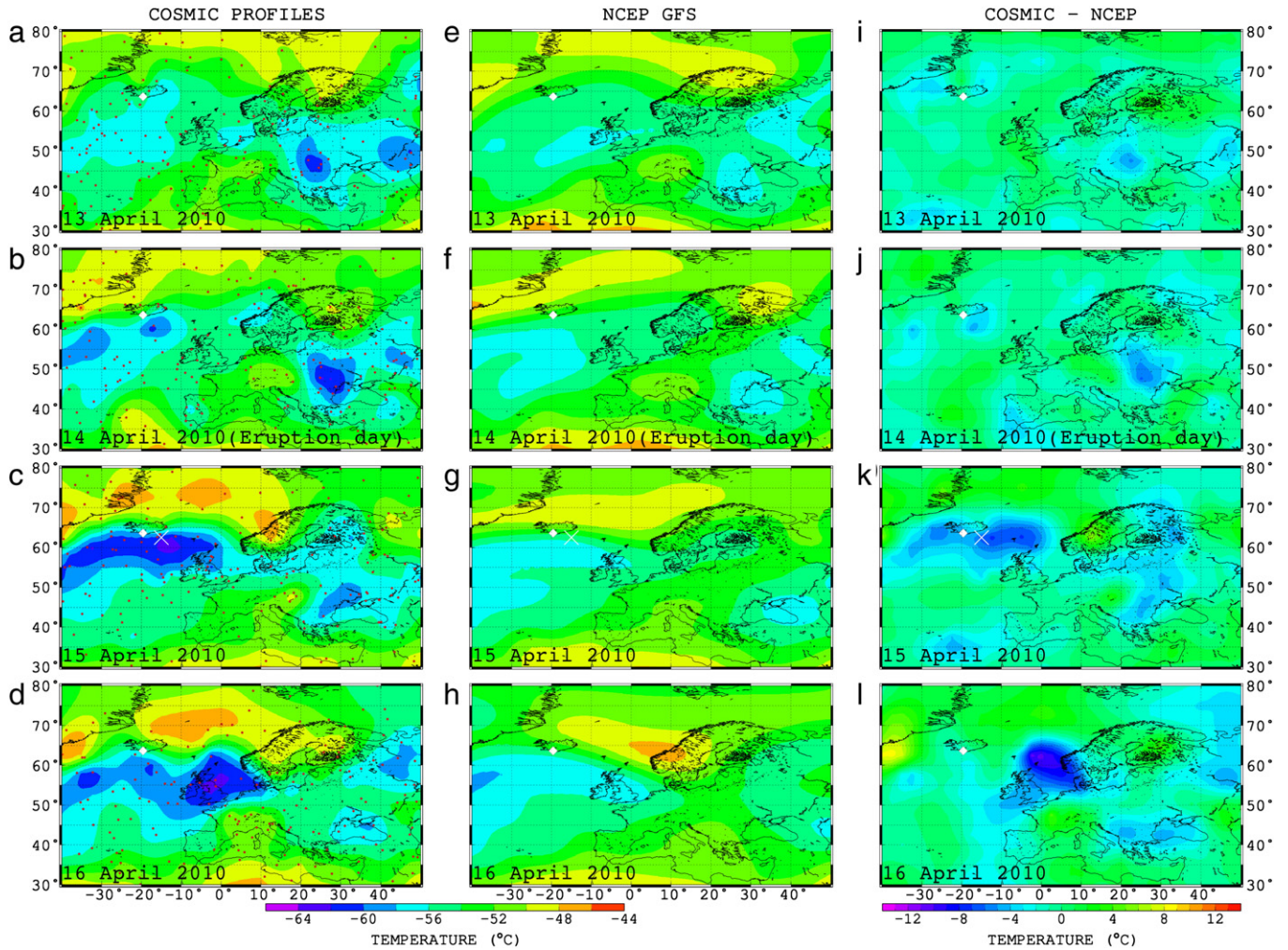


Fig. 1. (a) Aerosol optical depths derived from MODIS with the Terra satellite during 14–15 April 2010, in the Eyjafjallajökull eruption. (b) Same image from the Aqua satellite during 4–6 June 2011, in the Puyehue eruption. Yellow diamonds indicate locations of the studied volcanoes. (For interpretation of the references to color in this figure legend, the reader is referred to the web version of this article.)



**Fig. 2.** Daily average temperature distributions on the 250 hPa plane from the FS3/C profiles (red dots) for (a) 13, (b) 14, (c) 15, and (d) 16 April 2010. (e–h) Daily average temperature distributions from the NCEP GFS model. Forecasts are calculated from the initial values at 00:00 UTC on 13 April. (i–l) Difference between the FS3/C analysis and the NCEP GFS model forecast. The location of the Eyjafjallajökull volcano is shown on each map as a white diamond. Crosses in (c), (g), and (k) are the location of the temperature profile shown in Fig. 4a. (For interpretation of the references to color in this figure legend, the reader is referred to the web version of this article.)

days after the eruption), April, 2010. Fig. 2a–d are those inferred by the FS3/C observations. Before the eruption (Fig. 2a), temperature ranged between  $-54^{\circ}\text{C}$  and  $-50^{\circ}\text{C}$  around the volcano located near the southern edge of Iceland. On the eruption day (Fig. 2b), the southern side of Iceland began to be covered with cold air mass (below  $-54^{\circ}\text{C}$ ) extending E–W. On the next day of the eruption (Fig. 2c), cold part became more conspicuous on the SE side of the volcano. It drifted eastward on the following day (Fig. 2d).

Fig. 2e–h shows daily average temperatures forecasted by the NCEP GFS model on the 250 hPa layer. They generally agree with the FS3/C data in Fig. 2a–d. However, the forecasted temperature fields lack the cold air mass as shown in Fig. 2c, d.

Fig. 2i–l shows the differences between the observed (Fig. 2a–d) and the forecasted temperatures (Fig. 2e–h). The observation and the model agree well before the eruption (Fig. 2i). After the eruption, negative anomalies developed on the western and eastern sides of the volcano (Fig. 2k). Because the forecast started at 00:00 UTC on the previous day of the eruption, such differences would reflect the influence of the eruption.

The distribution of the negative temperature anomalies agrees well with the aerosol distribution observed by MODIS satellite (Fig. 1a). The largest temperature anomaly of  $-7$  to  $-8^{\circ}$  spatially coincides with the plume. It drifted eastward from 15 to 16 April (Fig. 2k–l).

### 3.3. Temperature anomaly: Puyehue

Fig. 3 shows observed and modeled temperature fields in the 2011 Chilean eruption case, derived in a similar way to Fig. 2. They show daily average temperature distributions from 3 to 6 June, 2011. The observations show that a low temperature region extended from the Antarctic Peninsula to the southern Chile throughout the studied period (Fig. 3a–d). However, the cold region in the NCEP GFS model (Fig. 3e–h) is distributed somewhat differently from the observations. For example, the relatively cold region is observed to have reached 35S on the eastern side of the volcano (Fig. 3a), but it remained within a higher latitude region in the model (Fig. 3e).

Temperature deviations of the observation from the model are shown in Fig. 3i–l. Unlike the case of the Eyjafjallajökull eruption, temperature anomaly of  $-7$  to  $-8^{\circ}$  already existed at around 80W, 40S, upwind of Mt Puyehue on the previous day of the eruption (Fig. 3i), and it moved eastward on the eruption day (Fig. 3j). Obviously, this anomaly would not be of volcanic origin. However, from 5 June, the next day of the eruption, the negative anomalies spread eastward (Fig. 3k, l), and showed similar distributions to the ash plume from the MODIS satellite image (Fig. 1b). As a whole, however, post-eruption negative temperature anomalies are not as clear as in the Icelandic case. Insufficient meteorological observations in southern

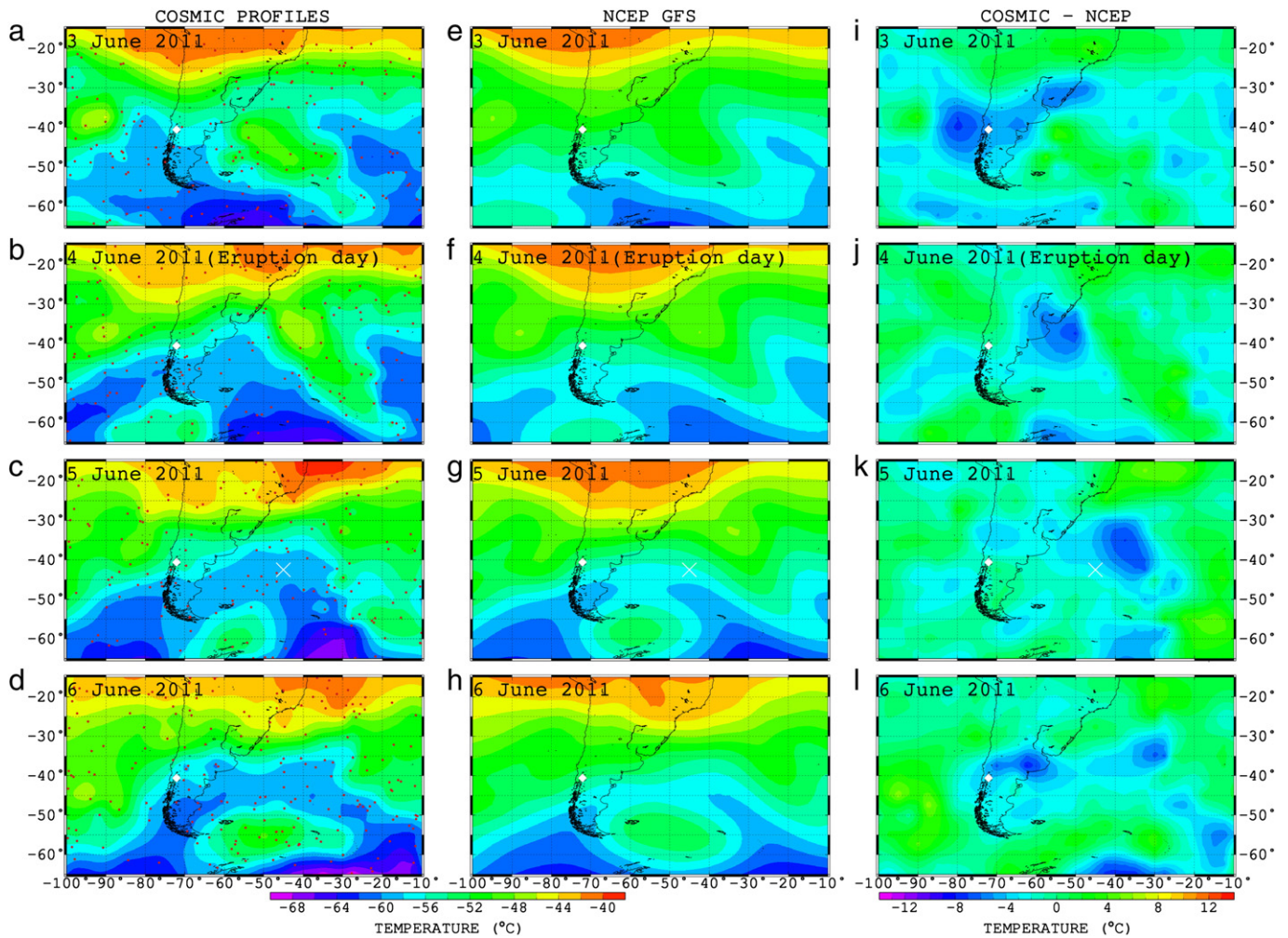


**Fig. 3.** Daily average temperature distributions at the 250 hPa plane from the FS3/C profiles (red dots) for (a) 13, (b) 4, (c) 5, and (d) 6 June 2011. (e–h) Daily average temperature distributions from the NCEP GFS model. Forecasts are calculated from initial value at 00:00 UTC on 3 June. (i–l) Difference between the FS3/C analysis and the NCEP GFS model forecast. The location of Mt Puyehue is shown on each map as a white diamond. Crosses in (c), (g), and (k) are the location of the temperature profile shown in Fig. 4b. (For interpretation of the references to color in this figure legend, the reader is referred to the web version of this article.)

hemispheric oceans may have affected precise forecasts of the NCEP GFS model in this region.

### 3.4. Comparison of temperature profiles

Fig. 4 compares the profiles of atmospheric temperature changes in these two eruptions. The daily mean vertical temperature profile of 15 April 2010, the next day of the Icelandic eruption, at 62.5N, 15.0W (Fig. 2k) is shown in Fig. 4a (interpolated using all available GPS-RO data). This figure also shows averaged profile within  $\pm 5$  days (i.e. 11–20 April) during 2007–2009 (i.e. years without eruption). Past profiles show fairly large natural variability (standard deviations are shown around the averaged profile). It should be emphasized that they are raw temperature profiles and not the deviations from the forecasted temperatures as discussed in the Section 3.2.

The 2011 Chilean case is shown in Fig. 4b, i.e. the profile on 5 June 2011, the next day of the eruption, at 42.5S, 45.0W (Fig. 3k), averaged profile within  $\pm 5$  days period during 2007–2010 and their SD.

In the 2008 eruption of the Chilean Chaiten volcano, Wang et al. (2009) found significant decreases in temperature at 14 km (lower stratosphere) and increases in temperature below 10 km (troposphere), in the downwind region of the volcano. Fig. 4 shows that significant decreases in temperature in tropopause and lower stratosphere also occurred after the 2010 Icelandic and 2011 Chilean eruptions. The height

of the largest temperature decrease is somewhat different between eruptions: it was  $\sim 10.5$  km in the former and  $\sim 11.5$  km in the latter. Such a difference may reflect the heights of the volcanic plumes (Table 1 and Fig. 4).

The temperature change in troposphere, however, was not so clear in the Icelandic case (Fig. 4a) as in the 2008 Chaiten case (Wang et al., 2009). On the other hand, temperature increase below 10 km was relatively clear in the 2010 Puyehue eruption (Fig. 4b).

As suggested by McCormick et al. (1995), two competing mechanisms, i.e. the reduction of solar radiation by the parasol effect and the absorption of long-wave radiation from the ground by the greenhouse effect, are responsible for the temperature changes associated with volcanic eruptions. Significant temperature decreases at higher altitudes seen in these three analyses certainly shows that volcanic plumes cool down atmosphere around the tropopause in region downwind of the volcano. However, temperature changes in the lower troposphere might be influenced by synoptic scale weather conditions (Wang et al., 2009) and then volcanic eruptions might not always exert the same influence.

## 4. Summary

By combining the FS3/C data and the NCEP GFS model forecast, we identified influences of volcanic eruptions in the atmospheric temperature profiles after two recent eruptions in Iceland and Chile.

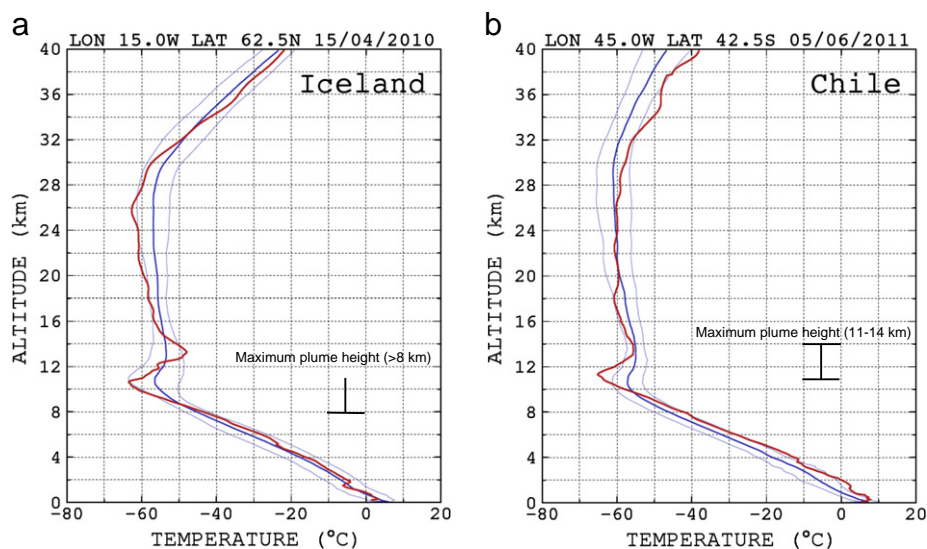


**Fig. 4.** (a) The red curve shows the daily mean temperature profile on 15 April 2010 (next day of the eruption) at 15.0W 62.5N, whose location is marked with X in Fig. 2c, g, k. The profile in dark blue shows average of the same region for the periods of 11–20 April during 2007–2009. Light blue curves show their standard deviation (SD). (b) The daily mean profile on 5 June 2011 at 45.0W 42.5S (X in Fig. 3c, g, k) (red curve), average profile within the period 1–10 June during 2007–2010 (dark blue curve), and their SD (light blue curves) shown in the same way as (a). The maximum plume heights (Table 1) are indicated in (a) and (b). (For interpretation of the references to color in this figure legend, the reader is referred to the web version of this article.)

**Table 1**

Three eruptions studied with GPS-RO.

Volcano	Location	Eruption date	VEI <sup>c</sup> (plume <sup>d</sup> )
Chaiten <sup>a</sup> (Chile)	42.8S 72.6W	02 May 2008	5 (20 km)
Eyjafjallajökull <sup>b</sup> (Iceland)	63.6N 19.6W	14 Apr 2010	4 (>8 km)
Puyehue-Cordón Caulle <sup>b</sup> (Chile)	40.6S 72.1W	04 Jun 2011	4 (11–14 km)

<sup>a</sup> Wang et al. (2009).

<sup>b</sup> This study.

<sup>c</sup> Volcanic explosivity index.

<sup>d</sup> Maximum plume height.

Negative post-eruptive temperature anomalies on the 250 hPa plane were found in the former. However, in the latter eruption, they were not so clear due possibly to the difference in accuracies of the forecasted temperature fields. By comparing the temperature profiles in the downwind location of these eruptions, we found that significant temperature decreases occurred at ~10.5 and ~11.5 km altitude in the former and the latter cases, respectively. These results generally agree with Wang et al. (2009), but revealed some diversity in the temperature modifications by volcanic eruptions.

## Acknowledgments

We thank two anonymous reviewers whose comments significantly improved the paper.

## References

- Anthes, R., et al., 2008. The COSMIC/FORMOSAT-3 mission: early results. *Bulletin of the American Meteorological Society* 89, 313–333.
- Global Volcanism Program, 2010. Eyjafjallajökull, SI/USGS weekly volcanic activity report. 14 April to 20 April 2010. Smithsonian Inst., Washington, D. C.
- Global Volcanism Program, 2011. Puyehue-Cordón Caulle, SI/USGS weekly volcanic activity report, 1 June to 7 June 2011. Smithsonian Inst., Washington, D. C.
- Hajj, G.A., et al., 2004. CHAMP and SAC-C atmospheric occultation results and inter-comparisons. *Journal of Geophysical Research* 109, D06109 <http://dx.doi.org/10.1029/2003JD003909>.
- Huang, C.-Y., Kuo, Y.-H., Chen, S.-H., Vandenberghe, F., 2005. Improvements in typhoon forecasts with assimilated GPS occultation reflectivity. *Weather and Forecasting* 20, 931–953.
- McCormick, M.P., Thomason, L.W., Trepte, C.R., 1995. Atmospheric effects of the Mt Pinatubo eruption. *Nature* 373, 399–404.
- Wang, K.-Y., Lin, S.-C., 2007. First continuous GPS soundings of temperature structure over Antarctic winter from FORMOSAT-3/COSMIC constellation. *Geophysical Research Letters* 34, L12805 <http://dx.doi.org/10.1029/2007GL030159>.
- Wang, K.-Y., Lin, S.-C., Lee, L.-C., 2009. Immediate impact of the Mt Chaiten eruption on atmosphere from FORMOSAT-3/COSMIC constellation. *Geophysical Research Letters* 36, L03808 <http://dx.doi.org/10.1029/2008GL036802>.
- Wickert, J., 2004. Comparison of vertical refractivity and temperature profiles from CHAMP with radiosonde measurements. *Sci. Rep.* 04–09. Dan. Meteorol. Inst., Copenhagen. 27 pp.